



Blockchain and 1D-CNN based IoTs for securing and classifying of PCG sound signal data

Zainab N. Al-Qudsy¹, Zainab Mahmood Fadhil², Refed Adnan Jaleel^{3,*}, Musaddak Maher Abdul Zahra⁴

¹ Department of Intelligent Medical Systems, University of Information Technology and Communications, Biomedical Informatics College

²Department of Computer Engineering, University of Technology – Iraq, Baghdad, Iraq,

³Department of Information and Communication Engineering, Al-Nahrain University, Baghdad, Iraq,

⁴Computer Techniques Engineering Department, Al-Mustaqbal University, Babil, Iraq

Emails: dr.zainab.n.yousif@uoitc.com; Zainab.M.Fadhil@uotechnology.edu.iq; iraq_it_2010@yahoo.com; musaddaqmahir@mustaqbal-college.edu.iq

Abstract

The Internet of Things (IoT) has accelerated with the introduction of powerful biomedical sensors, telemedicine services and population ageing are concerns that can be solved by smart healthcare systems. However, the security of medical signal data that collected from sensors of IoTs technology, while it is being transmitted over public channels has grown to be a serious problem that has limited the adoption of intelligent healthcare systems. This suggests using the technology of blockchain to create a safe and reliable heart sound signal (PCG) that can communicate with wireless body area networks. The security plan offers a totally dependable and safe environment for every data flowing from the back end to front-end. Also in this paper, to classify heart sound signals, we suggested a one-dimensional convolutional neural network (1D-CNN) model. The denoising autoencoder extracted the heart sounds' deep features as an input feature of 1D-CNN. To extract the detailed characteristics from the PCG signals, a Data Denoising Auto Encoder (DDAE) was used instead of the standard MFCC, the suggested model shows significant improvement. The system's benefits include a less difficult encryption algorithm and a more capable and effective blockchain-based data transfer and storage system.

Keywords: Blockchain; IoT; PCG; 1D-CNN

1. Introduction

In 2008, Satoshi Nakamoto developed blockchain technology to operate as Bitcoin's public transaction record. Due to the technology's reputation for reliability, it has been widely used in a variety of industries, including healthcare data management, insurance, and finance.

Using the blockchain, the authors in [1] suggested a solution called MedRec in 2016 to control who may view sensitive medical records. Benefiting specifically from the blockchain's decentralized nature, it manages confidentiality, authentication, data sharing, accountability, important things to keep in mind while working with Electronic Medical Records (EMRs).

Advantages of using the technology of blockchain into the storage and administration of biological and healthcare data are also explored by the authors of [2]. However, the publications did not take into account the practical conditions when IoT instruments are contained in the front-end.

Two different blockchain depend smart systems of healthcare with back-end and front-end solutions were presented by the authors in [3, 4]; the front end of [3] was built on top of a widespread social network, and [4] made use of a WBAN. Blockchain technology, as was previously said, may provide environment that depend on back-end of smart healthcare systems, the processing time and the maximum capacity in reaching consensus

with the front-end concerned are two of the biggest obstacles. Since each node in the network has the potential to act as a peer in the blockchain, each node must have access to sufficient computational and storage capabilities in order to maintain the distributed ledger and facilitate the consensus procedures. Even though hubs have superior hardware resources (typically, they are smartphones or tablets) in contrast to biological sensors, they still find it challenging and redundant to continuously process and store the entire ledger. As a result, this article proposes a system for smart healthcare using blockchain. This not only makes the back end more capable and faster, but also creates an environment where healthcare data can be transmitted and stored safely [5,6].

Due to the fast progress of advanced biomedical sensors, IoTs, and modern technologies of wireless communication, smart system of healthcare offer workable solutions to the issues of telemedicine services and population aging [7].

However, as physiological data concerns personal privacy, the issue of data security during information transmission on open networks has emerged as a major obstacle to the widespread adoption of intelligent systems of healthcare.

In this article, a blockchain-based intelligent healthcare system that interacts with wireless body area networks is presented.

Everything from the user's device to the server's storage is protected by the security protocol. The evaluation findings demonstrate the resistance to popular attack techniques and time savings of the piecewise linear chaotic map-based encryption scheme. The system's advantages include a simple encryption strategy, increased storage and transmission capacity, and increased efficiency thanks to the blockchain.

A heart sound recording is known as a phonocardiogram (PCG) signal representing the closure of the tricuspid and mitral valves, respectively, which results in the first (S1) and second (S2) heart sounds and the semilunar valves closing, respectively [8]. Evaluating the stethoscope-recorded PCG signal is crucial for early detection of cardiac disease, numerous efforts have been made, including the use of computer-aided techniques for the categorization of PCG signal abnormalities, and heart condition prediction system. In contrast, it was proposed in this work to create a device for collecting PCG signals that could segment the signal and assess cardiac conditions in two parties: healthcare and user professionals [9]. The PCG signals were first collected using a heart sound sensor, which was managed by an Arduino Uno microcontroller. Power spectral density and Fast Fourier transform were used on the signals to discover the range of frequency of the pathological and normal PCG. Pathological PCG signals were discovered to have a greater frequency than normal PCG signals. Additionally, the placement of the S1 and S2 peaks in pathological and normal PCG signals provided further evidence of the murmur's considerable difference [10]. In addition to the S1 and S2 peak locations, the PCG signals' power spectra were also recorded and kept in Amazon Web Services (AWS) as a cloud system, from which authorized users may get them at any time. Therefore, these results may help the e-health system, leading to a better way of life. Specifically, we put forth a model for a single-dimensional CNN, which, independently of the ECG, distinguishes between normal and pathological cardiac sound waves. The denoising autoencoder (DAE) technique was used to extract the heart sounds' deep characteristics, which were then used as the input feature of a one-dimensional convolutional neural network (1D CNN). The results if the experiment demonstrated that the model with deep features outperformed the model with mel-frequency cepstral coefficients in terms of anti-interference performance, and the suggested 1D CNN model outperforms the backpropagation neural network (BP) model in terms of classification F-score, Precision, and accuracy [11].

2. Materials and Methods

2.1 One-dimensional convolutional neural network

The deep characteristics of EEG sound waves were extracted using a DAE and fed into 1D convolutional neural networks (CNNs) in our research, and the signals were classified using a soft max classifier. Figure 1 depicts a system schematic of the entire setup. CNNs were first used for voice recognition in 2012 by Abdel-Hamid, who also described its fundamental structure, which alternated between pooling and convolution layers. When comparing the convolution kernel size with CNN layers, the latter is smaller. Even though language is often a 1D signal, the CNNs utilised for the speech recognition job are a 2D model. In Figure. 7, we see a diagram of a typical CNN structure.

The CNNs are made up of fully connected layers for creating semantic features and alternatively configured convolutional layers and pooling layers for feature extraction. Figure 1 depicts a conventional CNN and feature extraction method in two dimensions. For ease of usage, we refer to the convolutional layer and pooling layer as C and P, respectively, and the fully connected layer as F-C. Convolution kernels are a group of filters that are used to produce feature maps by iteratively processing the input [12, 13].

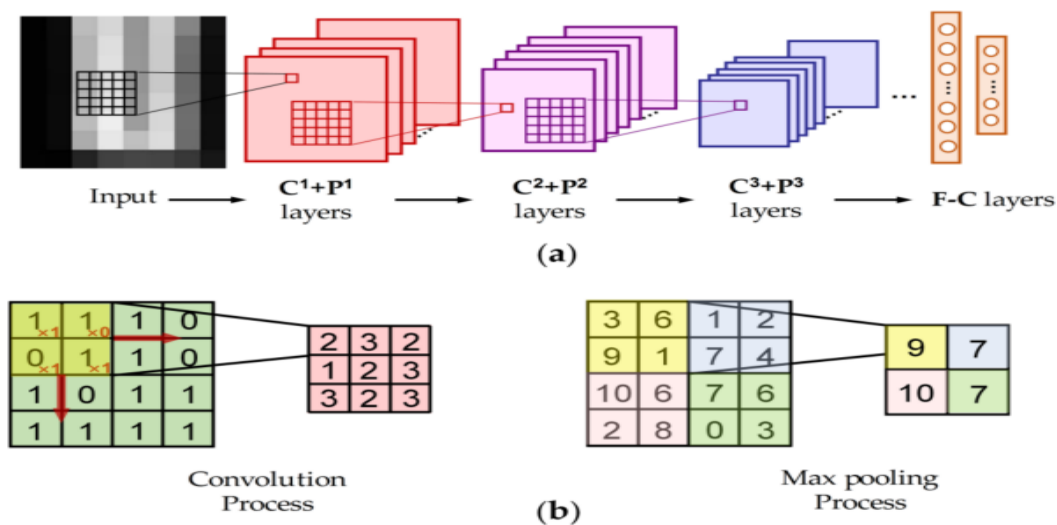


Figure 1 (a): The format of a standard CNN, (b) the process of max pooling (pooling size: 2, stride: 2) and of convolution (kernel size: 2×2).

All the network's building blocks—convolution kernel, feature map, etc.—are flat. Currently, when using CNNs to process 1D signals, the signal of 1D is often transferred to a space of 2D (for instance, one can transform a one-dimensional voice signal into a two-dimensional static feature map or a frequency-time feature). These 2D characteristics are then sent into the normal 2D Convolutional Neural Networks for Processing. Frame-by-frame analysis of speech, feature extraction, and columnar feature arrangement represent the conventional method for observing capability development and local characteristics of the long band signal. However, the two dimensions have distinct meanings; one is concerned with time domain properties, while the other is concerned with frequency characteristics. Since two dimensions have entirely distinct physical meanings, 2D CNNs are unable to adequately adapt to 1D speech features [14].

In this research, 1D audio signal features—specifically, the CNNs input of 1D vector—were exploited. Consequently, the characteristic map and convolution kernel inside the networks were likewise 1D, and the values of m_s , S_i , m_c , m_i , and C_i in the graph were all 1 [15].

For modelling the recognition of heart sounds, 1D CNNs were employed. Only the characteristics of the signal that were recovered from the automated encoder were used in the CNN input to create the first dimension.

Convolution layer's actual physical significance, which is analogous to a filter, is to extract a subset of relevant information from a convolution. The size and shape of the convolution kernel directly affect the networks performance. When convolution kernel's size is tiny, the input signal's correlation information is lost in the derived feature.

To extract additional characteristics, a convolution kernel of 1D that generally linked to the lengthy signal frames is utilised. The feature graph collected by the coiling layer will be sampled by the pooling layer. The maximum pool area value is chosen in this study as after pooling point. All characteristics were vectors of 1D that can be linked in a straightforward fashion.

To create an output with the same classes number, the whole connection layer was applied. The function of loss analogous to the classification cross entropy is implemented in the output layer to compute the prediction error. The BP is carried out to update the deviations and weights following forward propagation. As a result, the loss and inaccuracy are decreased.

2.2 Sample expansion

To evaluate the impact of 2-CNNs on PCG, their structures were reduced to their bare essentials: sampling layer, complete network layer, and convolution layer. The models of 2-DCNN were trained with the same number of layers. The transfer function was sigmoid, and 20 feature maps made up the convolution layer. Maximum pooling was employed in the pooling layer, and the stride was set at 2. The probability of posterior of each class was output by the softmax classifier. One auto encoder characteristic was extracted and utilised to ensure that the sonic signal was accurately described. The window for the heartbeat was pretreated. Traditional 1D CNNs' extracted MFCC coefficient was utilised as networks input and comparison of the deep characteristics obtaining a heart sound recording required a minimum of 5 s.

In this investigation, the signals were separated into 5 s chunks, and quite prevalent window smoothers was chosen [16]. To begin, rather than retrieve the complete record, we trained the classifier on subsamples to differentiate between "normal" and "pathological heart" sound signals. By increasing the size of the data and then combining the lengths of all the samples, the classifier not only increased the size of the total data but also decreased over fitting during network training [17].

3. Extraction of Features depend on the dAE

The goal of extraction for feature is to pull out the distinguishable parts of a signal. The MFCC is frequently utilised in speaker and automated voice recognition. It was first suggested around 1980, and it has been essential for speech recognition ever since [18]. The basis for analysis of the mel-frequency is the auditory perception of humans. The findings of the experiments demonstrate that the ear functions like a filter bank, selecting and highlighting specific frequency components. In other words, it only send signals at specific frequencies and outright rejects unwanted transmissions. Thus, even after applying these feature factors to the frequency and time domains, there is still a significant amount of information loss.

The audio stream is first framed in the MFCC method before being reshaped into tiny windows using the Hamming window. Each frame's spectrum is computed with the fast Fourier transform, and after that, a filter bank is used to weigh every spectrum.

Lastly, logarithmic and discrete cosine transformations were utilized to construct the MFCC vector. We resampled all of the signals to 16 kHz, and we used 40 filters with a filter order of 24 during feature extraction. Stride was 10 ms and the sample size was 25 ms (15 ms overlap). The acquisition environment for the sound of heart was also varied, and the signal itself was poor in relation to the noise. Because of this, the MFCC cannot adequately capture the characteristics of heart sounds as a parameter of a speech feature. In this paper, we used the network of DAE to gather the PCG signal characteristic parameters. The spectrogram of a heartbeat (shown in Figure 5b) provides a visual depiction of the signal's frequency spectrum as it evolves over time. We may intuitively detect the formants and characteristics of the phonemes in the signal by examining the time domain received data to create a time changing spectrogram.

it is possible to directly extract speech coding using the original speech signal's spectrogram data for feature identification if the unsupervised learning utilized to automatically encode the speech feature. As previously indicated, to determine the heart's sound signal's characteristics, we employed the DAE network, which accepts a spectrogram as input. The auto encoder works on the premise that given an input (x), it is possible to derive a target output (y) by applying a weighting (W) and a mapping (b) in the form of a sigmoid function or tanh function, and finally, by applying an inverse weighting (z), the target output may be recovered. Iteratively training (W, b) to reduce the function's error, or to make sure that z is as near to x as feasible, allows for perfect reconstruction. It is possible to express the x to y mapping procedure as follows:

$$M = \text{sigmoid}(Wx + b) \quad (1)$$

Its transfer function is a sigmoid ().The encoder is the name of this procedure. The transformation from message M to its reconstruction vector R is referred to as the decoding process.

$$R = \text{sigmoid}(W'y + b') \quad (2)$$

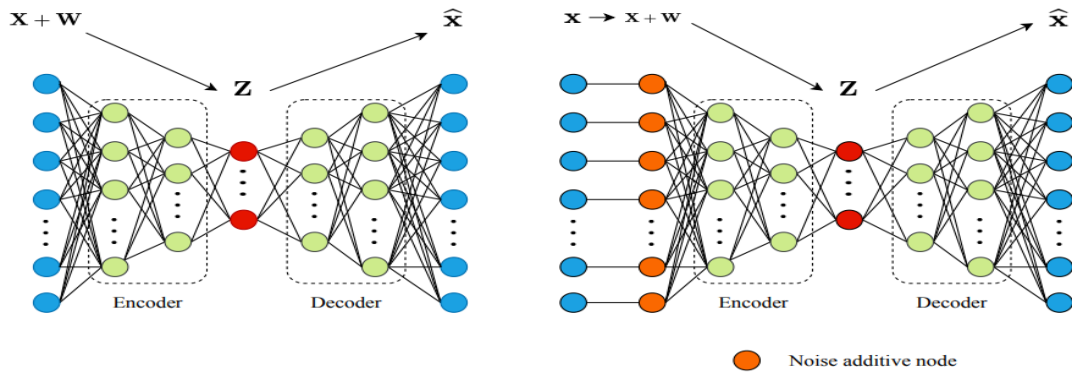
W stands for weight and b for bias. The encoder weight matrix $W' = WT$ may be left as the weight matrix W' , which can be transposed. Essentially, what is happening is a form of rebuilding. Following is the expression for the loss function (Cross entropy and difference Square):

$$L(xz) = \|x - z\|^2 \tag{3}$$

$$L_H(xz) = -\sum_{k=1}^s [x_k \log z_k + (1 - x_k) \log (1 - z_k)] \tag{4}$$

We used a DAE algorithm to extract features from the raw EEG audio data of all participants in this investigation. The deep network Vincent 08 presented the DAE, an extension of the auto encoder. The learnt encoder is made more robust and the model's generalisation ability is improved by introducing noise into the input data (the input network layer) to prevent over-fitting. The original data in the DAE can be recreated by training the samples with noise. It is possible to introduce noise by randomly setting some parts of the input signal to zero applying a binomial distribution with factors p and n (n is the number of pixels in the spectrogram, and p is 40%). A corrupted version of the input, in which the elements are randomly assigned to 0, is used to teach the DAE to rebuild a clean "repaired" input [19].

Error iterations are performed using the computed z and the original x to get a value for the missing x needed to calculate y. As a result, the network learns about the faulty data. When compared to non-destructive data training, this approach has the benefit of the damage data's training of the weight noise is pretty little and statistics on the damage minimising the gap between training and testing data. As seen in Figure 2, the robustness has increased [20].



4. Comparison of different convolution kernel shapes

The only difference between this method and [10] [11] is that we use an EEG dataset also the difference in kernel size. Input to a 1-DCNN model is a 1x256-dimensional vector. We develop 2-DCNN models similarly to 1-DCNNs and train them [11]. An average of 20 feature maps are convolutional layered into each model, and the function of transfer is sigmoid. The stride is 2 and the pooling layer uses maxpooling. The posterior probability of each class is calculated as the result using the softmax classifier. As an illustration, consider the five-layer 1-DCNN utilizing a convolution kernel size of 1x12, In Figure 3, the network structure is shown [10] [11].

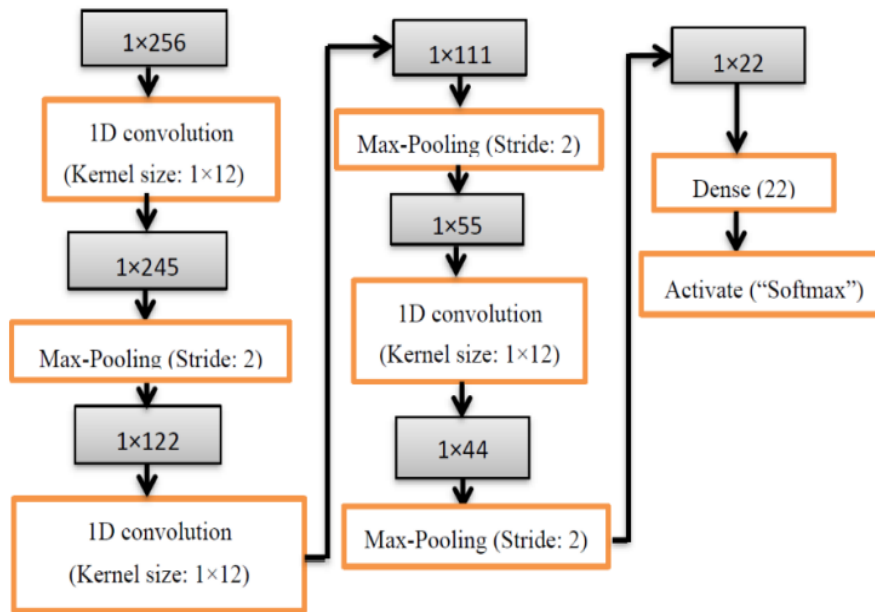


Figure 3: Structure of the neural network used in the suggested 1D convolutional model

The 2D convolution kernel is simplified to its 1D analogue by column expansion. To investigate how two CNNs perform in relation to the effectiveness of different convolution kernel shapes, both networks should use the same size convolution kernels, nevertheless it is important to modify the forms, so they accurately match the 1D and 2D representations [21].

Table 1 displays experimental data showing that, for a given convolution kernel size, the identification accuracy decreases as the convolution kernel size increases from 1D to 2D and around 2.5% is the highest amplitude (when the convolution kernel size is 39). The 1D CNNs maintain a recognition accuracy of around 0.01 ~ 0.03 greater than the 2D CNNs regardless of the convolution kernel shape.

Figure 10 demonstrates that the recognition accuracy is 89.75% when compared to other classification techniques, like as neural network of BP and this paper's approach improves recognition rates overall by about 7%. Like 1D CNNs, the BP neural network employs the same amount of weight factors. The HMM has six states, and three Gaussian distributions are used to approximate distribution of probability of the measured signal.

Chaotic systems exhibit the following traits: pseudo-randomness, initial value sensitivity, and ergodicity. As a result, theoretically, chaotic systems are related to one another and cryptography due to their innate structural similarities. While the chaotic systems sensitivity primarily depending on the beginning values chosen and the factors of structural system, the conventional encryption techniques security based on the key space size [22].

If the structural factors and the beginning value are altered, the chaotic sequence will take on a completely new form, and its orbit will be completely random. The chaotic map will iteratively diffuse across the phase space with the selection of the proper parameters. Chaotic encryption is reliably scrambled and disseminated because to the special mixing properties of chaotic systems.

It is critical to select suitable parameters in the system of digital chaotic to guarantee the system's chaotic dynamics. Only when the beginning parameters and values of system are adjusted to the proper values to achieve the chaotic state can the ergodicity of the system and unpredictability of orbits be satisfied. This is because some nonlinear systems are sensitive to started values [23].

5. Piecewise Linear Chaotic Map

The 1D discrete mapping known as PLCM has seen much study for its potential use in data encryption. Eq. 1 and Fig. 4 show its expression and associated figure, respectively.

$$y_{n+1} = \begin{cases} y_n/p, & y_n \in (0, p) \\ (y_n - p)/(1/2 - p), & y_n \in [p, 1/2) \\ (1 - y_n - p)/(1/2 - p), & y_n \in [1/2, 1 - p) \\ (1 - y_n)/p, & y_n \in [1 - p, 1) \end{cases} \quad (5)$$

It has been shown that PLCM is a parameterized expression of the form $P(0, 1/2)$. The PLCM is perpetually in a chaotic state in this domain $y_0 \in (0, 1)$ is the stated value of chaos. As offered in Figure 5, The PLCM-obtained sequence is normally dispersed in the interval when the structural factor p has an effective value $(0, 1)$. More significantly, the sequence produced when the starting value of $y(0)$ or p marginally changes is likewise considerably vary as a result of chaos's sensitivity of the starting value [24, 25].

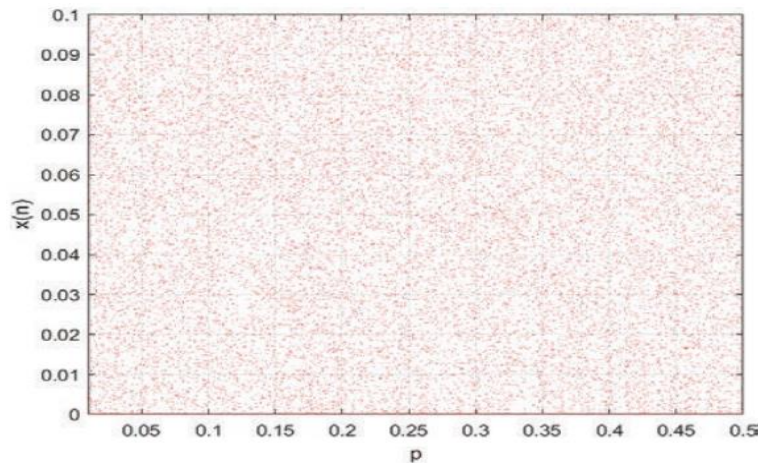


Figure 4: PLCM Scatter diagram.

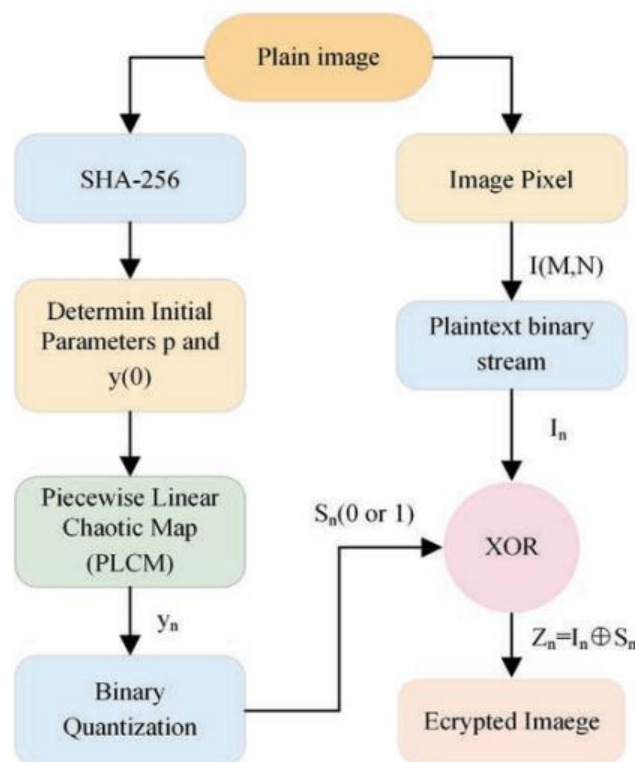


Figure 5: WBAN encryption method based on PLCM.

6. Key Generation

SHA-256 is extremely sensitive to the beginning conditions, just as chaotic systems. The hash value will be significantly altered even by a single pixel change in the plaintext. The SHA-256 hash value is utilized as a perturbation of the chaos's initial value to increase the algorithm's sensitivity to plaintext. Plaintext photos and gathered physiological data, such as PCG signals, are used as the hash function's input.

Each pixel's value is swapped out with the amplitude of a randomly chosen to point in the PCG signal, which shown in Figure 6. For a image that is 512 x 512 in size, 512 replacements can be made in each of the 512 squares, It significantly heightens the challenge of decrypting the key. Based on Eq. 2, we can see that the 256-bit hash H value is broken down into 32 segments, everyone is 8 bits in length.

It should be emphasised that each H will be displayed as integer data and will have a length of 8 bits, $H_i \in [0,255]$, $i = 1, 2, \dots, 32$. After applying Eq. 3 to the encryption keys y' and p' , we get the chaotic starting value. The interference of hash values will be amplified in a chaotic environment, altering the entire hash sequence [26, 27].

$$H = H_1, H_2, \dots, H_{32} \quad (6)$$

$$\begin{cases} y(0) = y' + \text{mod} \left(\frac{H_1 \oplus H_2 \oplus \dots \oplus H_{16}}{2560}, 1 \right) \\ p = p' + \text{mod} \left(\frac{H_{17} \oplus H_{18} \oplus \dots \oplus H_{32}}{2560}, 1 \right) \end{cases} \quad (7)$$

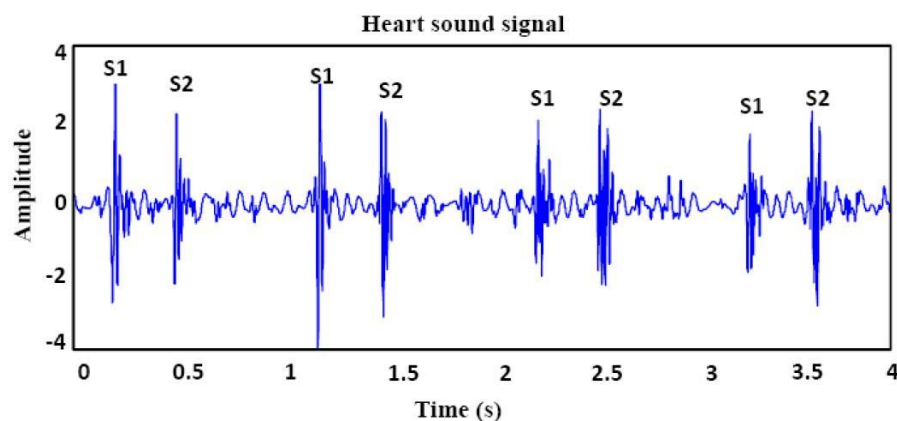


Figure 6: PCG Signal

7. Comparison of different features

To demonstrate that the extraction of feature approach employed in this work is better to the conventional features of MFCC, we carried out several sets of contrast trials. Table 2 provides a summary of the findings of the experiments. Table 2 demonstrates that the deep features in this article's extraction have good recognition rates, as a result, it can be concluded that the retrieved features are effective in blocking out unwanted sounds and adjusting to the unique qualities of each individual network. Figure 7 and Figure 8 show the comparison of 1D-CNN and 2D-CNN in accuracy and F score. Figure 9 offers the Evaluation of deep sound feature and MFCC correctness.

8. Comparison of several network layer counts

We take use of the suggested 1D-CNNs and expand them into two-layer CNNs by adding another neural network layer. This gives us better results. Convolutional and pool layers coexist in the structure of CNN. Layers of pool and convolution are inserted. The output is obtained once all the layers are joined. We contrast how the network performs at various layer depths. No matter how many layers are added to a network, we see no improvement in performance. Table 3 displays the experimental outcomes. The results show that the convolution layer increment has improved the signal's ability to identify the samples in the present study. Figure 10 offers the

comparison of F score with deep sound features and MFCC. Figure 11, and Figure 12, shows the 1D-CNN and 2D-CNN comparison in accuracy and F score.

9. Evaluation of the Trustworthy Blockchain

To assess the blockchain network architecture, The two blockchains were created using Hyperledger Fabric version 1.0, and Simple, transaction-submitting apps were developed using Node-RED. The design and implementation of the network on Hyperledger Fabric were made easier by the Hyperledger Fabric Composer framework. It was also useful in the development of a REST server, which in turn enabled the safe exposure of a transaction-submitting interface. The REST servers and Fabric blockchains used for the system assessment were all run within virtual machines running Ubuntu 16.04 LTS 64-bit. Within the VMs, Docker containers hosted the blockchain's central authority, ordering service, and peers.

The neighbourhood blockchain network was assessed on one virtual computer. This Vm served as a central node, collecting data from sensors, and submitting transactions to the neighbourhood blockchain. Also, it was far less frequent in sending transactions to the networked ledger. A review of the distant blockchain network was done in the second virtual computer.

In this setup, the virtual computer acted as a permanent decentralised storage for the data. location. A blockchain network may be modelled using the Composer framework with the asset's utilization, transactions, and participants. Whoever or anything participates in a blockchain network, transactions are ways to engage with assets, which services or products are tangible or intangible.

A patient is the sole sort of user on the local blockchain. Each patient is coupled with the patient's daily health records. The patient's daily health record asset can be updated by sensors sending blockchain transactions on their behalf.

Update daily health record is one sort of transaction that is used to add new values to A routine health record asset for a patient. The submission of this kind of deal occurs regularly; Every time a new measurement is made, a transaction with all the essential data is posted to the blockchain.

Multiple kinds of users can join the blockchain remotely, including emergency service, insurance company, government, medical center, doctor, pharmacy, and the household. The local blockchain networks' preferred main type is the household participant and facilitate the submission of transactions on behalf of a participant to a distant blockchain network. Once more, a health record is one of the assets; however, this is not a daily health record for a single patient; rather, it is a permanent record for a whole household. It must emphasize that the records are rarely up to date, as previously said, only includes data deemed important enough to permanently retain.

Like previous iterations, A permanent health record update transaction is accessible. This work is not intended to cover the other parties, assets, or transactions; thus, they will not be looked at. Finally, even if the hub belongs to the regional blockchain network, it only communicates with the distant blockchain network over a protected REST interface.

An illustration of how it works is that every second the sensor can transmit measurements to the hub. Once every minute, the node can issue a transaction to the neighbourhood ledger. After that, once each day, after reviewing the data on the nearby blockchain, the hub has the capability of generating a unique form of transaction that includes crucial information like the daily average, the frequency of solely the above- and below-criteria measurements. It might incorporate information from all house sensors and hubs. Next, the transaction is transmitted to the blockchain network remotely so that the patient's permanent health record may be updated.

Table 1: Hyper-parameter comparison of several convolutional kernels.

Kernel Size of CNN	Kernel Type of CNN	Kernel Shape of CNN	F-Score%	Accuracy%
12	1-DCNN	1×12	92.9	90.2
	2-DCNN	1×12	91.4	89.1
24	1-DCNN	1×24	94	91
	2-DCNN	2×12	93	90
39	1-DCNN	1×39	90.4	88.4
	2-DCNN	3×12	89	87.2
52	1-DCNN	1×52	89.4	87.1
	2-DCNN	4×12	88	85.9
60	1-DCNN	1×60	92.7	90.6
	2-DCNN	5×12	90.9	89

Table 2: 1D-CNN includes a comparison of the findings.

Kind of Features	Kernel Shape of CNN	F-Score%	Accuracy%
MFCC	1×12	92.4	91.4
Deep EEG Audio		94.1	92.1
MFCC	1×24	92.7	89
Deep EEG Audio		94	91.7
MFCC	1×39	94	89.4
Deep EEG Audio		95.4	90.1
MFCC	1×52	89.7	87
Deep EEG Audio		91.4	89.2
MFCC	1×60	92.8	90.6
Deep EEG Audio		94	92

Table 3: 1D-CNN model is the end result of the varied feature type convolutional layer.

Type of Features	Kernel Shape of CNN	F-Score%	Accuracy%
Three 1-DCNN	1×12	91.7	89
Five 1-DCNN		92	90.7
Three 1-DCNN	1×24	93.5	88.8
Five 1-DCNN		94.8	91.4
Three 1-DCNN	1×39	90.4	89
Five 1-DCNN		93.9	91
Three 1-DCNN	1×52	89.4	87
Five 1-DCNN		91.8	89.9
Three 1-DCNN	1×60	92	94.2
Five 1-DCNN		94	97.1

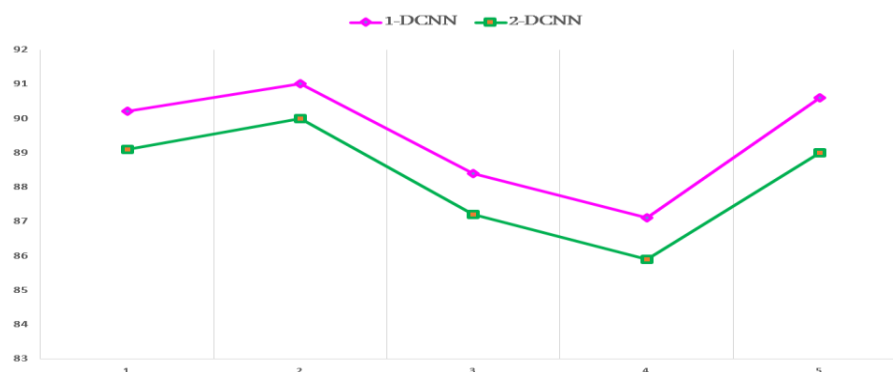


Figure 7: Comparison of the accuracy between 1D and 2D CNNs using various CNN kernel shapes.

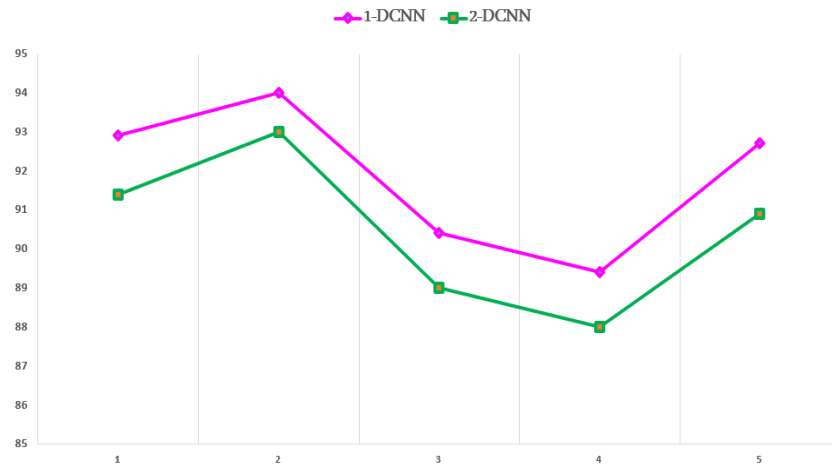


Figure 8: Contrasting 1D and 2D CNNs based on F scores and utilising various CNN kernel shapes.

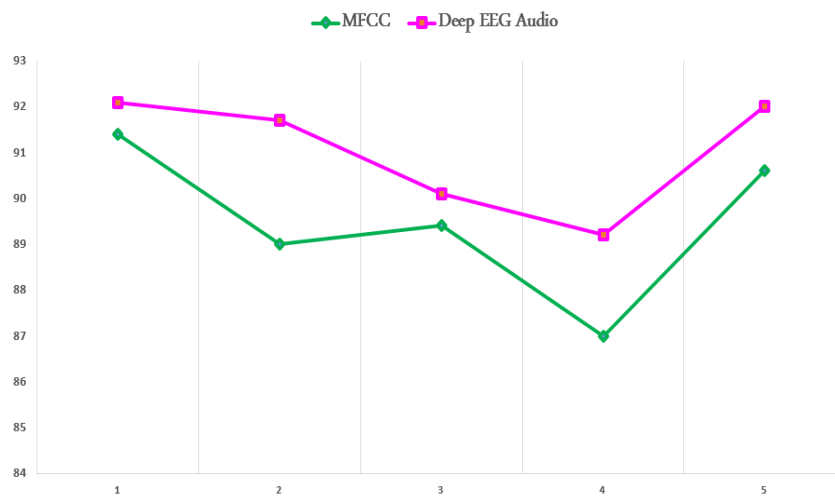


Figure 9: Evaluation of deep sound feature and MFCC correctness.

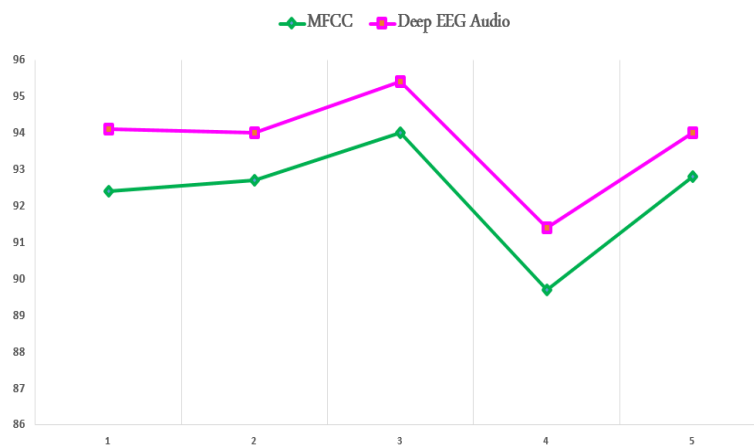


Figure 10: Comparison of F score with deep sound features and MFCC.

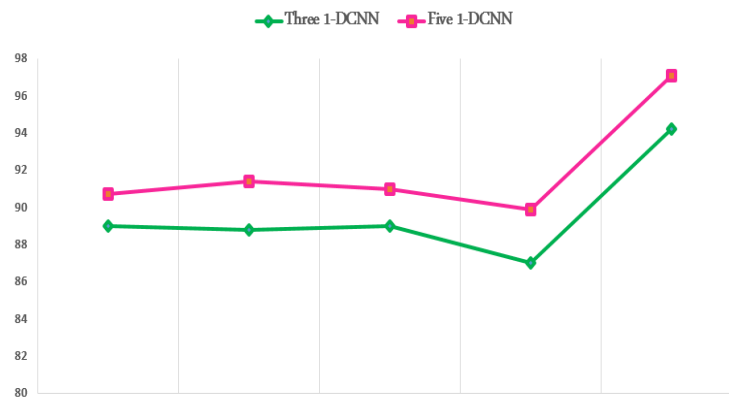


Figure 11: Accuracy evaluation Different CNN kernel sizes are used in 3-layer and 5-layer 1D convolutional.

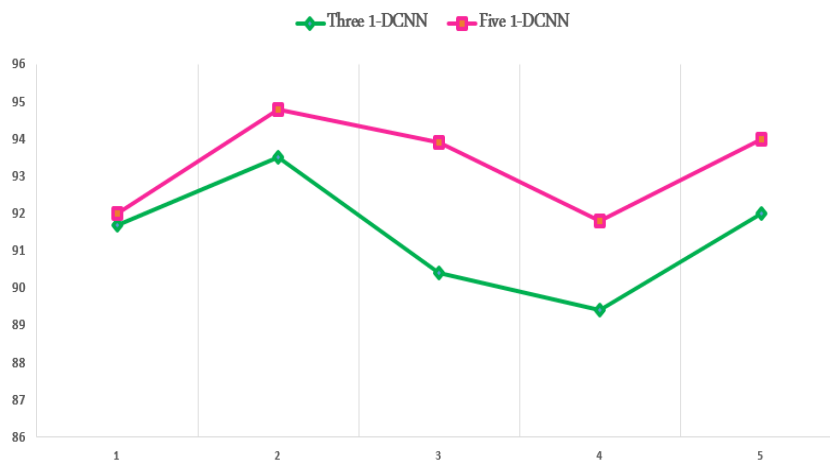


Figure 12: Compare F scores Different CNN kernel sizes are used in 3-layer and 5-layer 1D convolutional models.

10. Conclusions

This study suggested using a 1D-CNN to identify PCG signals instead of the more common MFCC. Data Denoising Auto Encoder (DDAE) was utilized to extract the detailed aspects of the sound signals. Therefore, a 7% improvement in accuracy over conventional MFCC is made. Using a 1D-CNN classifier, we successfully classified PCG sounds with high accuracy. In addition, this essay suggests a secure and trustworthy information security system that uses blockchain technology with chaotic encryption. It ensures the front-end data transfer between hubs and biological sensors in WBANs, through the suggestion of a chaotic encryption system based on PLCM, which not only can give sufficient encryption strength, but it has a less sophisticated structure than conventional encryption techniques. The primary benefit of the design is that it allows for significant increases in both overall maximum capacity and efficiency without requiring extensive changes to the design of any individual blockchain.

References

- [1] A. Azaria et al., "MedRec: Using Blockchain for Medical Data Access and Permission Management," 2016 2nd Int'l. Conf. Open and Big Data, Aug. 2016, pp. 25–30; <http://ieeexplore.ieee.org/document/7573685/>.
- [2] G. Zyskind, O. Nathan, and A. S. Pentland, "Decentralizing Privacy: Using Blockchain to Protect Personal Data," 2015 IEEE Security and Privacy Wksp., May 2015, pp. 180–84; <http://ieeexplore.ieee.org/document/7163223/>.
- [3] J. Zhang, N. Xue, and X. Huang, "A Secure System for Pervasive Social Network-Based Healthcare," IEEE Access, 2016.
- [4] J. Wang et al., "A Blockchain-Based eHealthcare System Interoperating with WBANs," Future Generation Computer Systems, Oct. 2019.
- [5] Wang, J., Fan, S., Alexandridis, A., Han, K., Jeon, G., Zilic, Z., & Pang, Y. (2021). A multistage blockchain-based secure and trustworthy smart healthcare system using ecg characteristic. *IEEE Internet of Things Magazine*, 4(3), 48-58.
- [6] H. Li, L. Deng, and Z. Gu, "A Robust Image Encryption Algorithm Based on a 32-bit Chaotic System," IEEE Access, vol. 8, 2020, pp. 30,127–51
- [7] G. Zyskind, O. Nathan, and A. S. Pentland, "Decentralizing Privacy: Using Blockchain to Protect Personal Data," 2015 IEEE Security and Privacy Wksp., May 2015, pp. 180–84; <http://ieeexplore.ieee.org/document/7163223/>.
- [8] Musa, M., Ibrahim, N., & Abd Rahman, N. U. (2021, November). Initial Development IoT-Based of Heart Sound Segmentation and Diagnosis System. In *2021 IEEE 19th Student Conference on Research and Development (SCOReD)* (pp. 257-261). IEEE.
- [9] Li, F., Liu, M., Zhao, Y., Kong, L., Dong, L., Liu, X., & Hui, M. (2019). Feature extraction and classification of heart sound using 1D convolutional neural networks. *EURASIP Journal on Advances in Signal Processing*, 2019(1), 1-11.
- [10] Lella, K. K., & Pja, A. (2021). Automatic COVID-19 disease diagnosis using 1D convolutional neural network and augmentation with human respiratory sound based on parameters: cough, breath, and voice. *AIMS Public Health*, 8(2), 240.
- [11] Li, F., Liu, M., Zhao, Y., Kong, L., Dong, L., Liu, X., & Hui, M. (2019). Feature extraction and classification of heart sound using 1D convolutional neural networks. *EURASIP Journal on Advances in Signal Processing*, 2019(1), 1-11.
- [12] T. Y. Lin, M. Maire, S. Belongie, J. Hays, P. Perona, D. Ramanan, P. Dollár, C. L. Zitnick, in *Computer Vision ? ECCV 2014*. Microsoft coco: Common objects in context, (2014), pp. 740–755. https://doi.org/10.1007/978-3-319-10602-1_48
- [13] Y. Li, M. Y. Liu, X. Li, M. H. Yang, J. Kautz, in *Computer Vision ? ECCV 2018*. A closed-form solution to photorealistic image stylization, (2018), pp. 468–483. https://doi.org/10.1007/978-3-030-01219-9_28
- [14] S. Jothilakshmi, V. Ramalingam, S. Palanivel, Unsupervised speaker segmentation with residual phase and MFCC features. *Expert Syst. Appl.* 36(6), 9799–9804 (2009)
- [15] Rajsekhar A.G., Real time speaker recognition using MFCC and VQ[J]. Department of Electronics & Communication Engineering National Institute of Technology Rourkela (2008)
- [16] A. P. Nair, S. Krishnan, Z. Saquib, MFCC based noise reduction in asr using kalman filtering. *Adv. Sig. Process* (2016)
- [17] L. Deng, M. L. Seltzer, D. Yu, et al., Binary coding of speech spectrograms using a deep auto-encoder[C]. Eleventh Annual Conference of the International Speech Communication Association (2010)
- [18] P. Vincent, H. Larochelle, Y. Bengio, P. A. Manzagol, in *Proceedings of the 25th international conference on Machine learning - ICML '08*. Extracting and composing robust features with denoising autoencoders (ACM Press, 2008). <https://doi.org/10.1145/1390156.1390294>
- [19] Liu, Y., Alzahrani, I. R., Jaleel, R. A., & Al Sulaie, S. (2023). An efficient smart data mining framework based cloud internet of things for developing artificial intelligence of marketing information analysis. *Information Processing & Management*, 60(1), 103121.
- [20] Ahmed, B. K. A., Mahdi, R. D., Mohamed, T. I., Jaleel, R. A., Salih, M. A., & Zahra, M. M. A. (2022). A novel secure artificial bee colony with advanced encryption standard technique for biomedical signal processing. *Periodicals of Engineering and Natural Sciences (PEN)*, 10(1), 288-294.
- [21] V. Giancarlo, C. A. Lage, V. Gianluca, F. Elia, Multivariate linear regression of high-dimensional fmri data with multiple target variables. *Hum. Brain Mapp.* 35(5), 2163–2177 (2014)
- [22] Juneja, A., & Marefat, M. (2018, March). Leveraging blockchain for retraining deep learning architecture in patient-specific arrhythmia classification. In *2018 IEEE EMBS International Conference on Biomedical & Health Informatics (BHI)* (pp. 393-397). IEEE.

- [23] Taralunga, D. D., & Florea, B. C. (2021). A blockchain-enabled framework for mhealth systems. *Sensors*, 21(8), 2828.
- [24] Nguyen Gia, T., Nawaz, A., Peña Querata, J., Tenhunen, H., & Westerlund, T. (2019, November). Artificial Intelligence at the Edge in the Blockchain of Things. In *International Conference on Wireless Mobile Communication and Healthcare* (pp. 267-280). Springer, Cham.
- [25] Kaur, H., Alam, M. A., Jameel, R., Mourya, A. K., & Chang, V. (2018). A proposed solution and future direction for blockchain-based heterogeneous medicare data in cloud environment. *Journal of medical systems*, 42(8), 1-11.
- [26] Husham Almkhtar, F., Abbas Ajwad, A., Kamil, A. S., Jaleel, R. A., Adil Kamil, R., & Jalal Mosa, S. (2022). Deep Learning Techniques for Pattern Recognition in EEG Audio Signal-Processing-Based Eye-Closed and Eye-Open Cases. *Electronics*, 11(23), 4029.
- [27] Al-Hashimi, M., Mohammed Jameel, S., Husham Almkhtar, F., Abdul Zahra, M. M., & Adnan Jaleel, R. (2022). Optimised Internet of Thing framework based hybrid meta-heuristic algorithms for E-healthcare monitoring. *IET Networks*.
- [28] Merkepci, M.; Sarkis, M. An Application of Pythagorean Circles in Cryptography and Some Ideas for Future Non Classical Systems. *Galoitica Journal of Mathematical Structures and Applications* **2022**.
- [29] Zayood, K., " On A Novel Generalization of The RSA Crypto-System", *Neoma Journal Of Mathematics and Computer Science*, 2023.